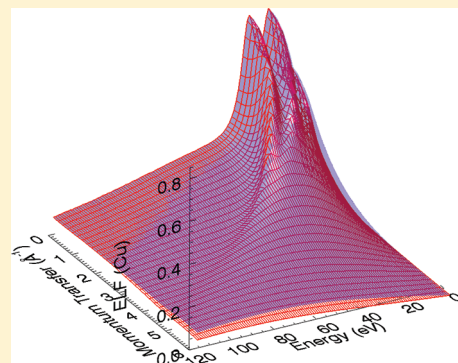


Electron Energy Loss Spectra and Overestimation of Inelastic Mean Free Paths in Many-Pole Models

Jay D. Bourke and Christopher T. Chantler*

School of Physics, University of Melbourne, Parkville, Victoria, 3010 Australia

ABSTRACT: We investigate established theoretical approaches for the determination of electron energy loss spectra (EELS) and inelastic mean free paths (IMFPs) in solids. In particular, we investigate effects of alternate descriptions of the many plasmon resonances that define the energy loss function (ELF), and the contribution of lifetime broadening in these resonances to the IMFP. We find that despite previously claimed agreement between approaches, approximations of different models consistently conspire to underestimate electron scattering for energies below 100 eV, leading to significant overestimates of the IMFP in this regime.



INTRODUCTION

The electron energy loss function is a prime quantifier of the interaction between a bulk material and a moving electron. It represents the probability of a scattering event in which the energetic electron transfers energy $\hbar\omega$ and momentum $\hbar q$ into the medium, via plasmon or single-electron excitations. Determination of the energy loss function is crucial for understanding elementary solid-state interactions and, in particular, is the principal determinant of the inelastic mean free path, a critical parameter in X-ray absorption fine structure,¹ X-ray photo- and auger-electron spectroscopy,² electron energy loss spectroscopy,³ imaging,⁴ and nanoscale structural determination.⁵ Through electron energy loss spectroscopy, the energy loss function provides detailed information regarding physical and electrical properties of materials⁶ and has even seen recent application in high profile work investigating the role of aerosols in climate change.⁷

It is standard to express the energy loss function of a given medium as the imaginary part of the negative inverse dielectric function, $\text{Im}[-1/\epsilon(q,\omega)]$. We define the real and imaginary parts of the energy- and momentum-dependent dielectric function as $\epsilon_1(q,\omega)$ and $\epsilon_2(q,\omega)$, so that we have

$$\text{Im}\left[\frac{-1}{\epsilon(q,\omega)}\right] = \frac{\epsilon_2(q,\omega)}{\epsilon_1^2(q,\omega) + \epsilon_2^2(q,\omega)} \quad (1)$$

General expressions for $\epsilon_1(q,\omega)$, $\epsilon_2(q,\omega)$, and $\text{Im}[-1/\epsilon(q,\omega)]$ can prove difficult to obtain for arbitrary solids, with intrinsically q -dependent theory claims typically limited to a few electronvolts above the Fermi level.⁸ First principles calculations may more readily be made, however, for the special case of a nearly free electron gas, in which electron interactions with a lattice potential are neglected.⁹ This result, referred to as the Lindhard equation for $\epsilon(q,\omega)$, can be used as a starting point for a general solid by implementing the statistical approximation.¹⁰ This

approximation treats the solid as a collection of small regions of definite charge density corresponding to nearly free electron gases. Accordingly, we can treat the energy loss function as a sum of Lindhard terms, where the Lindhard dielectric function is defined as follows:

$$\epsilon_L(q,\omega) = 1 + \frac{3\omega_p^2}{q^2 v_F^2} f \quad (2)$$

where

$$f = \frac{1}{2} + \frac{1}{8z} [1 - (z - u)^2] \ln\left[\frac{z - u + 1}{z - u - 1}\right] + \frac{1}{8z} [1 - (z + u)^2] \ln\left[\frac{z + u + 1}{z + u - 1}\right] \quad (3)$$

and

$$u = \frac{\omega}{qv_F} \quad (4)$$

$$z = \frac{q}{2q_F} \quad (5)$$

ω_p represents the plasma frequency of the nearly free electron gas, and v_F and q_F are the Fermi velocity and momentum, respectively. We can use eq 1 to determine the energy loss function (ELF) produced by each Lindhard term and sum together terms based on different ω_p 's, with different relative amplitudes. This allows us, in principle, to produce any arbitrary ELF at a given value of q .

The value of this approach arises from the availability of ELF data at $q = 0$ from either density functional theory¹¹ or, more

Received: October 20, 2011

Revised: February 6, 2012

Published: March 5, 2012

commonly, experimental techniques.¹² If we have an experimental (or theoretical) determination of the ELF, $\text{Im}[-1/\epsilon_{\text{exp}}(0,\omega)]$, we can determine the amplitudes, A_i , of the Lindhard terms following

$$\sum_i A_i \text{Im} \left[\frac{-1}{\epsilon_L(0,\omega;\omega_p=\omega_i)} \right] = \text{Im} \left[\frac{-1}{\epsilon_{\text{exp}}(0,\omega)} \right] \quad (6)$$

We can then use the Lindhard expression to determine $\epsilon(q,\omega)$ and $\text{Im}[-1/\epsilon(q,\omega)]$.

This approach is relatively simple due to the property of the Lindhard equation that it produces, for each component, a delta function in the ELF. This enables us to reproduce the experimental ELF exactly at $q = 0$, the optical limit, and makes the determination of the amplitude factors trivial. This is an example of a *many-pole* model; however, we will refer to it more specifically as a *partial pole* model, on the understanding that in practice a “real” plasmon resonance may, within this model, be represented by a summation of many terms. Despite differences in our expressions, this corresponds to an approach used by Tanuma et al.,¹³ whose IMFP results are among the most widely cited in the literature. Another example of a partial pole model is that used by Sorini et al.,¹⁴ who utilize a simpler dispersion relation in place of the Lindhard equation, and then use this to extend calculated optical ELFs to the region of finite momentum transfer.

The main alternatives to this kind of model are the *Drude* and *Mermin* approaches, which also employ a component-based fitting to an externally determined optical ELF. The principal difference is that these approaches include an additional lifetime broadening term, γ_i , for each plasmon or scattering resonance included in the ELF, which typically results in only a small number of terms being needed, of order 1–10. Such a representation implies that these models are explicitly many-pole models, but not partial pole models, as each component is designed to correspond with a particular physical excitation. Due to the classical basis of the Drude approach, the current work will focus solely on the Mermin approach, and on its relationship with the partial pole model. This investigation will reveal that the theoretical result for low and medium energy ELFs and inelastic mean free paths are not consistent and have not yet converged to a unique result, even for classic materials such as copper.

METHODS

The Mermin approach requires the addition of a broadening term γ to the Lindhard equation. One may naively suggest simply adding an imaginary component to the expression for u such that

$$u \rightarrow u' = \frac{\omega + i\gamma}{qv_F} \quad (7)$$

This indeed broadens the plasmon resonances. However, it is not an acceptable strategy as it does not preserve the local electron number in the ELF.¹⁵ This is evidenced by its breaking of the Kramers–Kronig sum rule.¹⁶ Instead, Mermin suggested an alternative extension of the Lindhard equation as follows:¹⁷

$$\epsilon_M(q,\omega) = 1 + \frac{(1 + i\gamma/\omega)[\epsilon_L(q,\omega+i\gamma) - 1]}{1 + (i\gamma/\omega)[\epsilon_L(q,\omega+i\gamma) - 1]/[\epsilon_L(q,0) - 1]} \quad (8)$$

This equation has several compelling properties, but most particularly it preserves the Kramers–Kronig sum-rule regardless of the value of γ , and also

$$\lim_{\gamma \rightarrow 0} \epsilon_M(q,\omega) = \epsilon_L(q,\omega) \quad (9)$$

So our partial pole model is explicitly a special case of the Mermin model, where $\forall_i \gamma_i = 0$. The Mermin model is not the only plausible broadening extension into q -space, but it is the most popular.

RESULTS

We can investigate the effect of the nonzero broadening in the Mermin model by examining the ELF produced by, in the simplest case, a prototype material with a one-component Mermin dielectric function, and comparing this to the results obtained using a partial pole representation with the same ELF in the optical limit. For this analysis we use a prototype function where our Mermin parameters are $\omega_p = 25$ eV, $\gamma = 25$ eV, and $A_i = 0.8$.

Figure 1 shows the difference in the q -dependent ELFs of the two models. Both approaches lead to an effective broadening of

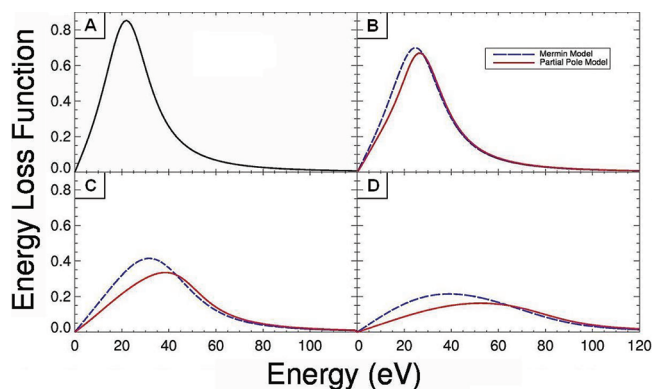


Figure 1. Evolution of a prototype one-component electron energy loss function from (A) the optical limit to (B) $q = 1 \text{ \AA}^{-1}$, (C) $q = 2 \text{ \AA}^{-1}$, and (D) $q = 3 \text{ \AA}^{-1}$. The dashed blue curve utilizes a Mermin model extension, peaking at lower energies than the solid red curve, which uses a partial pole representation. The two models coincide as the black curve in the optical limit.

the peak as the momentum transfer $\hbar q$ is increased. This broadening is greater when the one component Mermin picture is used, whereas the partial pole model predicts a thinner peak, with a higher-energy peak position. This effect is zero at the optical limit and increases monotonically for higher values of $\hbar q$. The variation is also greater for wider peaks, as is clear from the convergence of the Mermin and partial pole models in the limit of a delta peak ($\gamma = 0$). This difference has a considerable impact on the IMFP, λ .¹⁸

$$\lambda^{-1}(E) = \frac{\hbar}{a_0 \pi E} \int_0^{(E-E_F)/\hbar} \int_{q_-}^{q_+} \frac{1}{q} \text{Im} \left[\frac{-1}{\epsilon(q,\omega)} \right] dq d\omega \quad (10)$$

where a_0 is the Bohr radius. E_F is the Fermi energy, explicitly defined in this work as the energy corresponding to the electronic state with occupation probability of 0.5, and is measured relative to the bottom of the conduction band. q_{\pm} are

momentum-transfer limits, determined kinematically and given by

$$q_{\pm} = \sqrt{\frac{2mE}{\hbar^2}} \pm \sqrt{\frac{2m}{\hbar^2}(E - \hbar\omega)} \quad (11)$$

For our prototype material, we set the Fermi energy to zero and present the resulting IMFPs in Figure 2 using each ELF

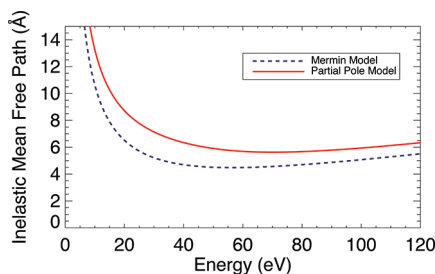


Figure 2. Electron inelastic mean free path of a prototype material defined by the optical energy loss function of Figure 1. The dashed blue curve uses a Mermin model for the extension to finite momentum transfer, whereas the solid red curve uses a partial pole model. Despite using identical optical data, these approaches give substantially different results, with variations of over 25% between 25 and 40 eV.

representation. The effect is dramatic, with deviations in excess of 25% between 25 and 40 eV. The two approaches become more consistent at very low energies, with the results converging as the energy closely approaches 0 eV, whereas the percentage difference slowly decreases, but does not disappear, as the energy increases well above 100 eV.

Because we are here considering only a single component Mermin spectrum, we can see that these results may be easily generalized. If, for an arbitrary Mermin type resonance of width γ_i , the ELF broadens at a greater rate with q than is seen with a partial pole representation, then this will happen for a general spectrum made up of many Mermin components. This will also correspond to a reduction in the resulting electron IMFP for any general material. The only variable in this effect will be the extent to which it occurs, which will be zero for spectra (or partial spectra) where $\gamma_i = 0$, and increasing for higher widths.

It is now profitable to consider explicitly the extent of the effect for a real material, for which we will choose copper as an example. For the optical ELF we utilize a widely cited experimental data set from Hagemann et al.¹² and a previously published Mermin-type fit to this data.¹⁹ These optical loss spectra are shown in Figure 3.

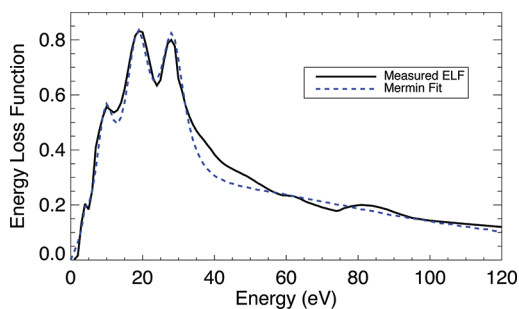


Figure 3. Comparison of the experimental optical energy loss function measured by Hagemann et al.¹² and a Mermin fit to this spectrum from Abril et al.¹⁹ The Mermin fit necessarily introduces errors in the inelastic mean free path; however in this case these errors are small relative to the effects of plasmon lifetime broadening.

DISCUSSION

The two spectra allow us to produce three separate IMFPs for copper: one using the Mermin approach from Abril et al.'s parametrization, one using a partial pole representation of this Mermin fit, and one using a partial pole representation of the original experimental data. The results are plotted in Figure 4

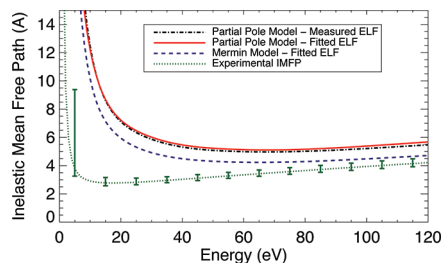


Figure 4. Calculations of the electron inelastic mean free path for copper. The dashed blue curve represents a Mermin model calculation, with optical data fitted to the experimental results of Hagemann et al.¹² The solid red curve is a partial pole calculation performed using the fitted optical data, and the dot-dashed black curve uses a partial pole model with the original experimental data. The dotted green curve is an experimental result, with three standard deviation uncertainties.²⁰

with energies relative to the Fermi energy, which we take as 7.0 eV for copper. Also shown is a recent measurement obtained from XAFS experiments.²⁰

The use of the Mermin terms in the q -extension results in IMFPs that are more than 15% lower for a large part of the energy range shown. This is a smaller effect than seen with the prototype material in Figure 2 but remains substantial. This is a particularly important result, as it is near certain that the true physical system consists of plasmon and other scattering resonances of varied lifetimes, some of which can be reasonably expected to be similar to those proposed by Abril et al. in their fitting. It can be inferred from the known optical spectrum that substantially broader peaks of high amplitude are not present, but it is quite reasonable to expect that the IMFP could lie anywhere between the partial pole (solid red curve) and Mermin (dashed blue curve) results shown in Figure 4. Further, our approach, as in previous work,^{15,21} utilizes characteristic broadening values for each plasmon resonance. As discussed by Egerton,⁶ real plasmons are more likely to instigate single electron excitations at higher momentum transfers, and therefore we should expect even shorter lifetimes, and thus greater broadening, as q is increased.

Our results are particularly striking when compared with the experimental data (dotted green curve). Agreement with experiment is improved significantly across the energy range shown, with the Mermin-based calculation coming very close to falling within the error bars at energies around 100 eV. At lower energies, below around 40 eV, experimental issues such as beam bandwidth and model dependence may cause errors in the measured data, and the theory is also quite sensitive to any errors in the optical ELF. We do find excellent evidence for our approach, however. We see the greatest agreement in the region where both the experimental and theoretical determinations should be considered most reliable, and we also see that such agreement is not apparent when the partial pole model is used.

These outcomes are somewhat different from some that have been reported previously. In a recent paper from Tanuma et al.,¹³ IMFP results from the Penn model, which is a partial pole

model, are compared with results produced by Denton et al.²¹ using a Mermin model. The materials compared are aluminum and gold, which is a particularly interesting comparison given that aluminum represents a very thin optical energy loss spectrum that should yield a similar IMFP irrespective of the model used. Conversely, gold possesses a broad loss spectrum where the effects of the wide Mermin peaks should be significant.

Unlike in our comparison, Tanuma et al. stated that the Mermin approach yields *higher* IMFPs than a partial pole approach for most of the energy range of interest to this paper, and that this holds for both aluminum and gold despite their starkly different optical loss spectra. The results are shown to converge well at high (kiloelectronvolts) energies for both materials. We attribute the conclusion of that paper to the use of an inconsistent version of eq 10 used by Tanuma et al. and by Denton et al. Though Tanuma et al. use an expression equivalent to ours, Denton et al. impose an extra condition on the range of the energy integral $d\omega$. They propose that the maximum range of integration should not exceed ω_{\max} , where

$$\omega_{\max} = \min\left(\frac{E}{2\hbar}, \frac{E - E_{\text{F}}}{\hbar}\right) \quad (12)$$

The extra limit of $E/2\hbar$ is claimed to be justified by the indistinguishability of the incident electron from an excited secondary electron. Though this is a valid argument for particular single electron excitations, it is not valid in general for excitations involving inner-shell electrons. This is because, under the approximation that all eigenstates are filled up to the Fermi level, such excitations require the transfer of a minimum binding energy. Therefore double-counting of transitions does not arise until well beyond the limit of $E/2\hbar$. More importantly, the truncated integration limit does not apply to the case of plasmon excitations, which are commonly the dominant cause of inelastic losses in the energy range of interest here. This is because a plasmon of well-defined energy is clearly a distinct entity to an energetic single electron, and is thus distinguishable. In any event, a meaningful comparison between the two models can only be achieved when the range of integration is consistent.

Another recent paper from de la Cruz and Yubero compared IMFP results from Mermin and partial pole models.²² This work utilized consistent integration limits, and therefore produced results qualitatively similar to our own, demonstrating the validity of our assessment that broadening must produce a reduction in IMFP values that spans all energies and materials. They also found a remarkable consistency in the magnitude of the effect, observing a linear relationship between IMFPs determined via Mermin and partial pole approaches for energies higher than 200 eV. Our work, focused on lower energies, demonstrates the breakdown of this relationship. We also improve on the analysis by explicitly using a Lindhard type partial pole model, rather than the simplified model used by de la Cruz and Yubero. A crucial advantage of this is that our approach satisfies eq 9, so that our results directly interrogate differences caused by the inclusion of finite broadening γ_i .

CONCLUSIONS

Our results raise the issue that the most popular approaches to theoretical determination of ELFs and IMFPs have surprising variation and are not consistent. In ideal cases this is likely to lead to discrepancies or errors of 25% or more.

Our results demonstrate that for a typical transition metal such as copper, significant uncertainty of 10–15% or more

exists in the theoretical IMFP for a range of energies below 100 eV. This uncertainty is greater for materials characterized by broad optical loss spectra, such as gold, despite previously claimed agreement between these approaches and relatively minor for nearly free-electron-like materials such as aluminum. In particular, the bulk of tabulated IMFPs may be expected to represent an approximate upper limit on the likely true values, due to the prevalence of either partial pole type models involving lossless plasmons, or models involving integration limits that are particularly inappropriate at low energies.

AUTHOR INFORMATION

Corresponding Author

*E-mail: chantler@unimelb.edu.au.

Notes

The authors declare no competing financial interest.

ACKNOWLEDGMENTS

We acknowledge Z. Barnea, C. Q. Tran, N. A. Rae,²³ and J. L. Glover, whose work and insights inspired the development of this research.

REFERENCES

- (1) Bourke, J. D.; Chantler, C. T.; Witte, C. *Phys. Lett. A* **2007**, *360*, 702–706.
- (2) Brown, M. A.; Faubel, M.; Winter, B. *Annu. Rep. Prog. Chem., Sect. C: Phys. Chem.* **2009**, *105*, 174.
- (3) Woodbridge, C. M.; Pugmire, D. L.; Johnson, R. C.; Boag, N. M.; Langell, M. A. *J. Phys. Chem. B* **2000**, *104*, 3085.
- (4) Kimoto, K.; Asaka, T.; Nagai, T.; Saito, M.; Matsui, Y.; Ishizuka, K. *Nature* **2007**, *450*, 702–704.
- (5) Muller, D. A.; Kourkoutis, L. F.; Murfitt, M.; Song, J. H.; Hwang, H. Y.; Silcox, J.; Dellby, N.; Krivanek, O. L. *Science* **2008**, *319*, 1073.
- (6) Egerton, R. F. *Rep. Prog. Phys.* **2009**, *72*, 016502.
- (7) Alexander, D. T. L.; Crozier, P. A.; Anderson, J. R. *Science* **2008**, *321*, 833.
- (8) Echenique, P. M.; Pitarke, J. M.; Chulkov, E. V.; Rubio, A. *Chem. Phys.* **2000**, *251*, 1.
- (9) Lindhard, J. *Dan. Mat. Fys. Medd.* **1954**, *28*, 8.
- (10) Penn, D. R. *Phys. Rev. B* **1987**, *35*, 482–486.
- (11) Kohiki, S.; Arai, M.; Yoshikawa, H.; Fukushima, S. *J. Phys. Chem. B* **1999**, *103*, S296–S299.
- (12) Hagemann, H.-J.; Gudat, W.; Kunz, C. *Deutsches Elektronensynchrotron Report SR-74/7 (unpublished)*, 1974.
- (13) Tanuma, S.; Powell, C. J.; Penn, D. R. *Surf. Interface Anal.* **2011**, *43*, 689.
- (14) Sorini, A. P.; Kas, J. J.; Rehr, J. J.; Prange, M. P.; Levine, Z. H. *Phys. Rev. B* **2008**, *74*, 165111–165118.
- (15) Planes, D. J.; Garcia-Molina, R.; Abril, I.; Arista, N. R. *J. Electron Spectrosc. Relat. Phenom.* **1996**, *82*, 23.
- (16) Barkyoumb, J. H.; Smith, D. Y. *Phys. Rev. A* **1990**, *41*, 4863.
- (17) Mermin, N. D. *Phys. Rev. B* **1970**, *1*, 2362.
- (18) Kwei, C. M.; Chen, Y. F.; Tung, C. J.; Wang, J. P. *Surf. Sci.* **1993**, *293*, 202–210.
- (19) Abril, I.; Garcia-Molina, R.; Denton, C. D.; Perez-Perez, F. J.; Arista, N. R. *Phys. Rev. A* **1998**, *58*, 357.
- (20) Bourke, J. D.; Chantler, C. T. *Phys. Rev. Lett.* **2010**, *104*, 206601–206604.
- (21) Denton, C. D.; Abril, I.; Garcia-Molina, R.; Moreno-Marin, J. C.; Heredia-Avalos, S. *Surf. Interface Anal.* **2008**, *40*, 1481–1487.
- (22) de la Cruz, W.; Yubero, F. *Surf. Interface Anal.* **2007**, *39*, 460.
- (23) Rae, N. A.; Chantler, C. T.; Barnea, Z.; de Jonge, M. D.; Tran, C. Q.; Hester, J. R. *Phys. Rev. A* **2010**, 1050.